2009 American Control Conference
Hyatt Regency Riverfront, St. Louis, MO, USA
June 10-12, 2009

A Control Allocation Approach for Energetic Swarm Control

R. Pedrami, S. Wijenddra, J. Baxter and B. W. Gordon

Abstract- **In this paper, a control allocation approach is developed for energetic swarm control. This new approach allows sliding control of swarm temperature, swarm center position, and swarm potential energy. Since the sliding control problem is highly over-actuated, a control allocation optimization problem can be formulated and solved including input saturation constraints. Application to a group of wheeled mobile robots is used to demonstrate the approach. For this class of systems, a low level trajectory controller based on dynamic feedback linearization is developed in order to improve the trajectory tracking performance of the individual swarm members. Together, these results allow energetic swarm controllers to be developed and applied for mobile robot systems with uncertainty and input saturation constraints.**

I. Introduction

Recent research in the area of swarm control has examined using swarm temperature as a controlled output variable in order to alter properties such as area coverage, swarm size and member velocities [1], [2]. This has been based on important contributions such as the development of stable attractor repulsion functions [3], the development of swarm stability characteristics such as controlling swarm size and cohesion as in [4] or the use of potential functions to direct and control swarm geometry as in [5]. In earlier work [6], a multi-output controller is proposed for the simultaneous control of the swarm temperature, swarm center position and swarm potential. The work is extended in [7] such that a control allocation algorithm and sliding manifold controller are used for implementation of the multi-output controller. Sliding approach provides a higher degree of robustness to the proposed control scheme compare to the feedback linearization method used in [6]. Most important, the control allocation algorithm is used to develop a stable high level multi-output controller for the overactuated swarm model. The control allocation method is more compatible for overactuated model comparing to [6].

Control allocation techniques are typically used for the control of overactuated systems, with much research having been done in the area of aircraft and ground vehicle control [8]. A straightforward technique to solve control allocation problems is the pseudo-inverse dynamics control law approach [7]. However, in order to consider constraints on the solution dictated by the mechanical system under control, methods have been developed to solve the control allocation optimization problem such as using a dynamic update law [9], or using sequential quadratic programming as in [10].

In the new approach developed in this paper, control allocation is used to combine the inputs from the swarm center position, swarm temperature, and swarm potential controllers. Initially an unconstrained pseudo-inverse approach is used. However in order to account for saturation effects of the swarm members, various optimization constraints need to be introduced. The SNOPT(c) [11] nonlinear programming software package was used in this application to provide a constrained optimal solution, allowing for the development of an operational envelope. In order to further improve the performance of the WMR swarm members under control, the outputs from the above high level swarm controller, are applied to a low level controller, which greatly improves the trajectory tracking for wheeled mobile robots. This low level controller was developed with the dynamic feedback linearization approach as provided in [12]. The proposed control scheme which combines high level controller and low level controller has more flexibility and robustness than the feedback linearization method proposed in [6]. Detailed results of a number of simulation cases are provided in the simulation results section.

II. Problem Statement

A. Swarm Theory Background

In this paper, we consider the control of a heterogeneous energetic swarm, made of M members moving in an n- dimensional space. The swarm motion is described by the following second order model represented as

$$m_i \dot{\mathbf{v}}_i = h_i(\mathbf{u}_i^{in} + \mathbf{u}_i^{ext}) - b_i \mathbf{v}_i + \mathbf{d}_i(t),\ \dot{\mathbf{x}}_i = \mathbf{v}_i \qquad (1)$$

where for each member i, $i = 1,2,\ldots,M$, the position is expressed as $\mathbf{x}_i \in \Re^n$, member velocity as $\mathbf{v}_i \in \Re^n$, m_i is the mass of the i^{th} member, $\mathbf{u}_i^{ext}$ is an external force, usually provided by a controller (as in our case) and $\mathbf{u}_i^{in}$ which represents the inter member repulsion-attraction force, h_i is the control coefficient, $-b_i \mathbf{v}_i$ represents the viscous damping and finally $\mathbf{d}_i(t)$ is a bounded disturbance on the i^{th} member. It is assumed that the disturbance is bounded as

$$\left\|\mathbf{d}_i(t)\right\| \le \beta_i,\ \ \beta_i > 0 \qquad (2)$$

The inter member repulsion-attraction force is given by (3)

R. Pedrami, S. Wijenddra, J. Baxter and B. W. Gordon are with Department of Mechanical and Industrial Engineering, Concordia University, 1455 de Maisonneuve Blvd. West, Montreal, Quebec, H3G 1M8, CANADA (phone: (514) 848-2424 ext. 7058; fax: (514) 848-3175; (e-mail: {rpedrami& wijenddra}@yahoo.com, j_baxt@sympatico.ca, and bwgordon@encs.concordia.ca,).

$$\mathbf{u}_i^{in} = -\sum_{j=1, j\neq i}^{M}\left[g_a^{ij}\left(\left\|\mathbf{x}_i-\mathbf{x}_j\right\|\right)-g_r^{ij}\left(\left\|\mathbf{x}_i-\mathbf{x}_j\right\|\right)\right](\mathbf{x}_i-\mathbf{x}_j) \quad (3)$$

where the repulsion force g_r^{ij} and the attraction force g_a^{ij} between members i and j are given by (4)

$$g_r(\|\mathbf{y}\|)=\frac{A}{\|\mathbf{y}\|^2},\ g_a(\|\mathbf{y}\|)=\frac{B}{\|\mathbf{y}\|} \quad (4)$$

where $A, B \in \Re^+$ and the norm is the Euclidean norm. The repulsion function is unbounded which ensure inter-agent collision avoidance. Cohesive behavior of the swarm is ensured to some degree with the inter-individual attraction function. The repulsion function is more dominant in short distance than the attraction function. Finally, we define certain fundamental swarm properties such as the weighted swarm center position $\bar{\mathbf{x}} \in \Re^n$ and weighted swarm center velocity $\bar{\mathbf{v}} \in \Re^n$ by (5).

$$\bar{\mathbf{x}}=\frac{\sum_{i=1}^{M}\bar{\omega}_i\mathbf{x}_i}{\sum_{i=1}^{M}\bar{\omega}_i},\ \bar{\mathbf{v}}=\frac{\sum_{i=1}^{M}\bar{\omega}_i\mathbf{v}_i}{\sum_{i=1}^{M}\bar{\omega}_i},\quad \bar{\omega}_i \geq 0 \text{ for any } i. \quad (5)$$

The swarm temperature $T \in \Re$ is defined as

$$T(\mathbf{v})=\frac{1}{M}\left(E_k(\mathbf{v})-E_b(\bar{\mathbf{v}})\right) \quad (6)$$

where E_k and E_b in (7) refer to the swarm weighted kinetic and the swarm weighted bulk energy respectively.

$$E_k(\mathbf{v})=\frac{1}{2}\sum_{i=1}^{M}\tilde{\omega}_i\left\|\mathbf{v}_i\right\|^2,\ E_b(\mathbf{v})=\frac{1}{2}\left(\sum_{i=1}^{M}\tilde{\omega}_i\right)\left\|\bar{\mathbf{v}}\right\|^2 \quad (7)$$

where $\tilde{\omega}_i$ is a positive weight coefficient for any i. The final variable introduced is a potential field force which is used to ensure swarm cohesion. A centrally connected potential function $J \in R$ is developed as in (8)

$$J=\frac{1}{2}\sum_{i=1}^{M}\alpha_i\left\|\mathbf{x}_i-\bar{\mathbf{x}}\right\|^2,\ \alpha_i \geq 0 \text{ for any } i. \quad (8)$$

where α_i is the connection weight. Physically, this can be interpreted as the case in which each agent is connected to the swarm center.

B. Energetic Swarm Control

The swarm model can be viewed as a combined dynamic of all individual members. Suppose a combined position vector $\mathbf{x} \in \Re^{nM}$, a combined velocity vector $\mathbf{v} \in \Re^{nM}$ and a combined control input vector $\mathbf{u} \in \Re^{nM}$ as :

$$\begin{aligned}\mathbf{x}&=({\mathbf{x}_1}^T,\ldots,{\mathbf{x}_M}^T)^T\\ \mathbf{v}&=({\mathbf{v}_1}^T,\ldots,{\mathbf{v}_M}^T)^T\\ \mathbf{u}&=({\mathbf{u}_1^{ext}}^T,\ldots,{\mathbf{u}_M^{ext}}^T)^T\end{aligned} \quad (9)$$

The n-dimensional swarm model proposed by (1)-(4) can be rewritten in a more compact form as:

$$\dot{\mathbf{x}}=\mathbf{v}$$
$$\dot{\mathbf{v}}=\mathbf{F}(\mathbf{x},\mathbf{v})+\mathbf{G}\left(\frac{h_1}{m_1},\frac{h_2}{m_2},\cdots,\frac{h_M}{m_M}\right)\mathbf{u}+\mathbf{D}(t)$$

where

$$\mathbf{F}(\mathbf{x},\mathbf{v})=\left[F_i(\mathbf{x},\mathbf{v})\right]_{i=1,\ldots,M}=\left[-\frac{h_i}{m_i}\left(\sum_{j=1,j\neq i}^{M}\left[\frac{A(\mathbf{x}_i-\mathbf{x}_j)}{\left\|\mathbf{x}_i-\mathbf{x}_j\right\|}-\frac{B(\mathbf{x}_i-\mathbf{x}_j)}{\left\|\mathbf{x}_i-\mathbf{x}_j\right\|^2}\right]\right)-\frac{b_i}{m_i}\mathbf{v}_i\right] \quad (10)$$

$$\mathbf{G}\left(\frac{h_1}{m_1},\frac{h_2}{m_2},\cdots,\frac{h_M}{m_M}\right)=diag\left[\frac{h_1}{m_1}\mathbf{I}_{n\times n}\quad\frac{h_2}{m_2}\mathbf{I}_{n\times n}\quad\cdots\quad\frac{h_M}{m_M}\mathbf{I}_{n\times n}\right]$$

$$\mathbf{D}(t)=\left[\mathbf{d}_i(t)\right]_{i=1,\ldots,M}$$

where $diag(\cdot)$ is block diagonal matrix with $n-$dimensional identity matrix $\mathbf{I}_{n\times n}$ as its diagonal elements. The control outputs are the weighted swarm center position, swarm temperature and potential function. Finally, the combined output vector can be constructed from equations (5), (6) and (8) as

$$\mathbf{y}(\mathbf{x},\mathbf{v})=\begin{bmatrix}\bar{\mathbf{x}}\\ T\\ J\end{bmatrix}=\begin{bmatrix}\mathbf{y}_1(\mathbf{x})\\ y_2(\mathbf{v})\\ y_3(\mathbf{x})\end{bmatrix},\ \mathbf{y} \in \Re^{n+2} \quad (11)$$

The swarm model given by (9)- (11) construct Multi Input Multi Output (MIMO) control problem. Then, the behavior control of the energetic swarm can be achieved by solving the proposed nonlinear MIMO system. The next step is to find the reduced output dynamic. This can be achieved by differentiation of each output until one input appears; the number of differentiation shows the relative degree of each output. The reduced dynamic can be shown as:

$$\ddot{\mathbf{y}}_1=\frac{\partial\bar{\mathbf{v}}}{\partial\mathbf{v}}\dot{\mathbf{v}}=\frac{\partial\bar{\mathbf{v}}}{\partial\mathbf{v}}\mathbf{F}(\mathbf{x},\mathbf{v})+\frac{\partial\bar{\mathbf{v}}}{\partial\mathbf{v}}\mathbf{G}\mathbf{u}+\frac{\partial\bar{\mathbf{v}}}{\partial\mathbf{v}}\mathbf{D}(t) \quad (12)$$

$$\dot{y}_2=\frac{\partial T}{\partial\mathbf{v}}\mathbf{F}(\mathbf{x},\mathbf{v})+\frac{\partial T}{\partial\mathbf{v}}\mathbf{G}\mathbf{u}+\frac{\partial T}{\partial\mathbf{v}}\mathbf{D}(t) \quad (13)$$

$$\ddot{y}_3=\mathbf{v}^T\frac{\partial^2 J}{\partial^2 x}\mathbf{v}+\frac{\partial J}{\partial\mathbf{x}}\mathbf{F}(\mathbf{x},\mathbf{v})+\frac{\partial J}{\partial\mathbf{x}}G\mathbf{u}+\frac{\partial J}{\partial\mathbf{x}}\mathbf{D}(t) \quad (14)$$

Introducing new inputs such as:

$$\upsilon_c=\frac{\partial\bar{\mathbf{v}}}{\partial\mathbf{v}}\mathbf{G}\mathbf{u},\ \upsilon_T=\frac{\partial T}{\partial\mathbf{v}}\mathbf{G}\mathbf{u},\ \upsilon_J=\frac{\partial J}{\partial\mathbf{x}}\mathbf{G}\mathbf{u} \quad (15)$$

Therefore, the newly introduced input vector $\upsilon \in \Re^{n+2}$ is given as $\upsilon=(\upsilon_c{}^T,\upsilon_T,\upsilon_J)^T$. The new control input vector is denoted as virtual input. Substituting (15) into (12)-(14), the control problem is decomposed into three separate sub-control problem with respect to new control input:

$$\ddot{\mathbf{y}}_1=\frac{\partial\bar{\mathbf{v}}}{\partial\mathbf{v}}\mathbf{F}(\mathbf{x},\mathbf{v})+\upsilon_c+\frac{\partial\bar{\mathbf{v}}}{\partial\mathbf{v}}\mathbf{D}(t) \quad (16)$$

$$\dot{y}_2 = \frac{\partial T}{\partial \mathbf{v}}\mathbf{F}(\mathbf{x},\mathbf{v}) + \upsilon_T + \frac{\partial T}{\partial \mathbf{v}}\mathbf{D}(t) \tag{17}$$

$$\ddot{y}_3 = \frac{\partial}{\partial \mathbf{x}}\mathbf{v}^T\frac{\partial^2 J}{\partial^2 x}\mathbf{v} + \frac{\partial J}{\partial \mathbf{x}}\mathbf{F}(\mathbf{x},\mathbf{v}) + v_J + \frac{\partial J}{\partial \mathbf{x}}\mathbf{D}(t) \tag{18}$$

Since the proposed model (10) is linear with respect to control input $\mathbf{u}$, the reduced output dynamic is also linear with respect to newly introduced input vector $\boldsymbol{\upsilon} \in \Re^{n+2}$. Moreover, the above equation shows that the dynamic of $\mathbf{y}_1$, y_2 and y_3 are decoupled from each other with respect to virtual inputs $\boldsymbol{\upsilon}_c$, υ_T and υ_J .As a result, the swarm control algorithm can be broken into two stages. In the first stage, virtual control inputs $\boldsymbol{\upsilon}_c$, υ_T and υ_J are independently calculated using the sliding mode controller respectively for the tracking control, temperature control and potential control.

We begin by discussing the swarm center trajectory tracking controller. Suppose $\bar{\mathbf{x}}_{des}$ is a desired trajectory of swarm center. First let $\bar{\mathbf{s}}$ be the sliding surface for the trajectory controller defined as

$$\bar{\mathbf{s}} = \dot{\tilde{\mathbf{x}}} + \bar{\boldsymbol{\lambda}}\tilde{\mathbf{x}} \tag{19}$$

where $\tilde{\mathbf{x}} = \bar{\mathbf{x}} - \bar{\mathbf{x}}_{des}$ is the tracking error vector and $\boldsymbol{\lambda}$ is a strictly positive constant. Now the virtual controller $\boldsymbol{\upsilon}_c \in \Re^n$ for the tracking is derived as

$$\boldsymbol{\upsilon}_c = -\left(\boldsymbol{\varsigma} + \boldsymbol{\lambda}\dot{\tilde{\mathbf{x}}} - \ddot{\bar{\mathbf{x}}}_{des}\right) - \mathbf{k}_c sat(\bar{\mathbf{s}}/\varepsilon_c) \tag{20}$$

where $\mathbf{k}_c$ is the $n \times n$ diagonal matrix of positive constant gain terms and $\boldsymbol{\varsigma}$ is defined as

$$\boldsymbol{\varsigma} = \left(\sum_{i=1}^{M}\frac{\bar{\omega}_i}{m_i}h_i\mathbf{u}_{in}^i - \sum_{i=1}^{M}\frac{\bar{\omega}_i}{m_i}b_i\mathbf{v}^i\right)\Bigg/\sum_{i=1}^{M}\bar{\omega}_i \tag{21}$$

$sat(\cdot)$ is the saturation function and ε_c is the thickness of the boundary layer.

Next the temperature controller is developed. The sliding surface for the temperature is defined as

$$s_T = T(\mathbf{v}) - T_{des} \tag{22}$$

where T_{des} is desired temperature. The virtual controller $\upsilon_T \in \Re$ for the temperature controller is calculated as

$$\upsilon_T = -\left(\frac{\sigma + \psi}{M} - \dot{T}_{des}\right) - k_T\, sat\left(\frac{s_T}{\varepsilon_T}\right) \tag{23}$$

where k_T is a positive constant gain term, σ is given as

$$\sigma = \frac{1}{2}\left(\sum_{i=1}^{M}h_i\frac{\tilde{\omega}_i}{m_i}(u_i^{in})^T\mathbf{v}_i\right) - \frac{1}{2}\left(\frac{\sum\tilde{\omega}_i}{\sum\bar{\omega}_i}\right)\bar{\mathbf{v}}^T\left(\sum_{i=1}^{M}h_i\frac{\bar{\omega}_i}{m_i}\mathbf{u}_i^{in}\right) \tag{24}$$

ψ is defined as

$$\psi = \frac{1}{2}\bar{\mathbf{v}}^T\left(\frac{\sum\tilde{\omega}_i}{\sum\bar{\omega}_i}\right)\left(\sum_{i=1}^{M}\frac{\bar{\omega}_i}{m_i}b_i\mathbf{v}_i\right) - \frac{1}{2}\sum_{i=1}^{M}\left[(\mathbf{v}_i)^T\frac{\tilde{\omega}_i}{m_i}b_i\mathbf{v}_i\right] \tag{25}$$

ε_T is the thickness of the boundary layer.

Finally the potential force controller is developed. The sliding surface for the potential controller is given as

$$s_{\bar{J}} = \dot{J} + \lambda(J - J_{des}) \tag{26}$$

where J_{des} is desired potential function. The virtual controller $\upsilon_J \in \Re$ for the potential energy is calculated as:

$$\upsilon_J = -\left(\xi + \lambda(\dot{J} - \dot{J}_{des}) - \ddot{J}_{des}\right) - k_J\, sat\left(\frac{s_J}{\varepsilon_J}\right) \tag{27}$$

where k_J is a positive constant gain. Term ξ is given as

$$\begin{aligned}\xi = &\sum_{i=1}^{M}\alpha_i(\mathbf{v}_i - \bar{\mathbf{v}})^T(\mathbf{v}_i - \bar{\mathbf{v}}) + \\ &\sum_{i=1}^{M}\left(\alpha_i\frac{h_i}{m_i}(\mathbf{x}_i - \bar{\mathbf{x}}) - \frac{\bar{\omega}_i}{m_i}h_i\boldsymbol{\chi}\right)^T\mathbf{u}_i^{in} - \\ &\sum_{i=1}^{M}\left(\alpha_i\frac{b_i}{m_i}(\mathbf{x}_i - \bar{\mathbf{x}}) - \frac{\bar{\omega}_i}{m_i}b_i\boldsymbol{\chi}\right)^T\mathbf{v}_i\end{aligned} \tag{28}$$

ε_J is the thickness of boundary layer and $\boldsymbol{\chi}$ is defined as

$$\boldsymbol{\chi} = \sum_{j=1}^{M}\alpha_j(\mathbf{x}_j - \bar{\mathbf{x}})\Bigg/\sum_{j=1}^{M}\bar{\omega}_j \tag{29}$$

Full detailed equations as well as the choice of gains and boundary layer thicknesses for each sub-controller are found in [7], which are omitted here.

Then in the second stage the actual force inputs are calculated from virtual inputs. The relation between virtual inputs and actual inputs are given by (15) which can be rewritten in a matrix format as

$$\begin{aligned}&\mathbf{B}\mathbf{u} = \begin{bmatrix}\mathbf{B}_c\\ \mathbf{B}_T\\ \mathbf{B}_J\end{bmatrix}\mathbf{u} = \begin{bmatrix}\boldsymbol{\upsilon}_c\\ \upsilon_T\\ \upsilon_j\end{bmatrix} = \boldsymbol{\upsilon} \quad \text{where}\\ &\mathbf{B}_c = \frac{\partial\bar{\mathbf{v}}}{\partial\mathbf{v}}\mathbf{G},\ \mathbf{B}_T = \frac{\partial T}{\partial\mathbf{v}}\mathbf{G},\ \mathbf{B}_J = \frac{\partial J}{\partial\mathbf{x}}\mathbf{G}\end{aligned} \tag{30}$$

where $\mathbf{B} \in \Re^{(n+2)\times nM}$ is the control effectiveness matrix. It is composed of three block control effectiveness matrices: $\mathbf{B}_c$ is the $n \times nM$ control effectiveness matrix associated to the virtual control input $\boldsymbol{\upsilon}_c \in \Re^n$, $\mathbf{B}_T$ and $\mathbf{B}_J$ are the $nM-$dimensional control effectiveness row vector associated to virtual control inputs $\upsilon_T \in \Re$ and $\upsilon_J \in \Re$ respectively. Please refer to [7] for the definition of each term as a function of $\mathbf{x}$ and $\mathbf{v}$.

The linear system of equation (30) has more than one solution. As a result, choice of actual inputs is not unique. This shows the fact that the overall proposed model is overactuated. In such a case, infinite solution exists. Hence a control allocation procedure is required to find the best solution which fits within the objective and limitation of the problem. Since the relation between virtual and actual input are linear, a linear control allocation algorithm can be used to solve the problem.

Now approaching the system as a control allocation problem we define the optimization problem as

$$\min_{\mathbf{u}}\frac{1}{2}\mathbf{u}^T\mathbf{W}\mathbf{u},\ \text{subject to}\ \mathbf{B}\mathbf{u} = \boldsymbol{\upsilon} \tag{31}$$

where $\mathbf{W} \in \Re^{nM \times nM}$ is a weighting matrix. The objective function is given by the quadratic function of the actual control inputs. The proposed allocation algorithm searches for a choice of actual inputs with minimum control effort. Initially a pseudo-inverse method as expressed in (32) is used to solve the control allocation problem.

$$\mathbf{u} = \left(\mathbf{W}^{-1}\mathbf{B}^T(\mathbf{B}\mathbf{W}^{-1}\mathbf{B}^T)^{-1}\right)\boldsymbol{\upsilon} \tag{32}$$

However this approach was not able to account for the effects of input saturation or other constraints.

C. Saturation

In order to account for saturation on the inputs from the control allocation result the following inequality constraints (33) can be incorporated into the allocation algorithm as follows:

$$\begin{aligned} &\min_{\mathbf{u}} \frac{1}{2}\mathbf{u}^T\mathbf{W}\mathbf{u}, \text{ subject to} \\ &\mathbf{B}\mathbf{u} = \boldsymbol{\upsilon} \\ &\mathbf{u}_{i\min} \le \mathbf{u}_i \le \mathbf{u}_{i\max},\ i = 1,2,\ldots M \end{aligned} \tag{33}$$

Now the above control allocation problem (33) with input saturation is solved using the SNOPT [11] optimization solver instead, replacing the pseudo inverse method of (32). However there is a threshold limit for the $\mathbf{u}_{i\min}, \mathbf{u}_{i\max}$ terms, otherwise the answer for the allocation problem will be not feasible i.e. (30) cannot be satisfied. That mean $\mathbf{u}_{i\min}, \mathbf{u}_{i\max}$ should be above a threshold value such that the allocation problem would be feasible. Also the maximum value of $\mathbf{u}_{i\min}, \mathbf{u}_{i\max}$ will be determined by the physical limits of the actuator. The threshold value depends on various factors such as initial condition, desired trajectory $\bar{\mathbf{x}}_{des}$, desired temperature T_{des} and desired potential energy J_{des}. In this paper, the goal is to estimate the value of $\mathbf{u}_{i\min}, \mathbf{u}_{i\max}$ that can be used for the steady state phase. The steady state threshold limits do not depend on initial condition. The threshold limits for the general transient response of the system is a subject of the future research.

The motion of the center of the cluster is not the key issue in terms of swarm behavior in comparison to temperature and potential energy. As a result, the dependency of saturation limits on steady state temperature and potential energy is studied. This can be achieved by assuming fixed trajectory of swarm center throughout all simulations. The regulation problem for temperature and potential energy is studied first then the results are generalized for a tracking case. The threshold value of $\mathbf{u}_{i\min}, \mathbf{u}_{i\max}$ are calculated experimentally at different operating conditions over the domain

$$5.0 \le T \le 20.0 \tag{34}$$

$$5.0 \le J \le 20.0 \tag{35}$$

It is important to note that all simulations are performed under the same initial condition. A surface plot of how the threshold value of $\mathbf{u}_{i\min}, \mathbf{u}_{i\max}$ varies with respect to temperature and potential terms is shown in Fig. 1.

Surface plot shows that the threshold limits are larger at higher temperature. This can be physically justified. Swarm has more kinetic energy at higher temperature. Therefore, maintaining swarm at higher level of kinetic energy requires more control effort. For instant, suppose a case in which the environment is viscous that is $b_i \neq 0$ for any i, having more velocity needs more control effort to overcome viscosity ψ-term in (25). Increase in dominant ψ-term makes virtual controller (23) larger. Finally, control allocation should assign larger values by accepting a larger saturation limit when virtual controller (23) gets larger. On the other hand, surface plot shows that threshold limits are getting larger at lower value of potential energy. This can be physically justified by the fact that lower level of potential energy introduces swarm with smaller size. Swarm of smaller size results in smaller inter-individual distance. At short distance, the unbounded inter-individual repulsion is more dominant than constant inter-individual attraction see (4) as mentioned in section II so members tend to repulse each other. Potential controller needs to put more effort to keep the members within a desired short distance. The following physical phenomena can be justified mathematically through (27) to (29) in a similar manner as temperature. The trend how a saturation threshold varies with respect to value of potential function highly depends on the choice of inter-individuals potential function.

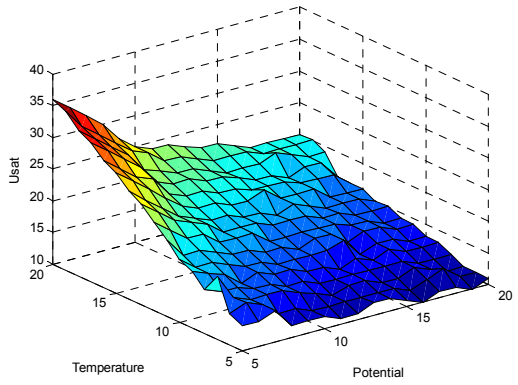

Fig.1 Minimum saturation limit w.r.t temperature and potential

Let $\mathbf{u}_{sat\min}$ be the minimum feasible value of $\mathbf{u}_{i\max}$. As mentioned, the major factors affecting $\mathbf{u}_{sat\min}$ were the operating conditions of the swarm T, J. The feasible operating region of the swarm is given by U_{sat} as

$$\mathbf{u}_{sat\min}(T, J) \le U_{sat} \le \mathbf{u}_{sat\max} \tag{36}$$

where $\mathbf{u}_{sat\max}$ is the physical saturation limit of the swarm inputs. In general $\mathbf{u}_{sat\min}$ is a nonlinear function. However, based on the result of numerous simulations, the following approximate lower bound on the operating region was obtained as

$$\mathbf{u}_{sat\min} \le c_0 + c_1 T + c_2 J \tag{37}$$

where c_0, c_1 and c_2 are determined from simulations over a number of different operating conditions over the domain (34)-(35). The coefficients were found to be $c_0 = 12.0$, $c_1 = 1.45$, $c_2 = -0.20$. Also the approximate

operating constraint below will also satisfy the operating constraint in (36).

$$c_0 + c_1 T + c_2 J \le \mathbf{u}_{sat\max} \tag{38}$$

The saturation threshold in steady state phase for a more general case in which the tracking problem for temperature and potential energy is desired is a given by nonlinear function:

$$\mathbf{u}_{sat\min}\left(T, J, \dot{T}, \dot{J}, \ddot{J}\right) \tag{39}$$

However, based on the result of numerous simulations, the following approximate lower bound on the operating region was obtained as

$$\mathbf{u}_{sat\min} \le c_0 + c_1 T + c_2 J + c_3 \dot{T} + c_4 \ddot{J} \tag{40}$$

It was found that the major factors affecting $\mathbf{u}_{sat\min}$ were the operating conditions of the swarm T, J and $\dot{T}$, $\ddot{J}$. Note that $\dot{T}$ and $\ddot{J}$ as of (23) and (27) has direct relation to υ_T and υ_J while the effect of $\dot{J}$ is less dominant. That's the reason that $\dot{J}$ is missing in a linear approximation.

III. Application To Wheeled Vehicle Systems

A. Low Level Controller

A low level controller is developed for each wheeled mobile robot (WMR) members to track a generated trajectory from high level controller. The proposed low level controller is used to track the center of the WMR as opposed to in [6,13] where the feedback linearization method is used to control the tip of a WMR. The kinematic equations of WMR agents are given by

$$\begin{pmatrix}\dot{x}_c & \dot{y}_c & \dot{\theta}\end{pmatrix} = \begin{pmatrix}v_c\cos\theta & v_c\sin\theta & \omega\end{pmatrix} \tag{41}$$

where v_c is the surge speed of the WMR, (x_c, y_c) denotes the position of the center of robot. The orientation of the robot is given by θ and ω is angular speed. Suppose the output of the swarm model (1) for the i^{th} member as $\mathbf{X}_{Out}^T = (x_i, y_i)$. Now, integrating with our high level controller, the input to the kinematic model (41) is the output from the swarm model. That is the kinematic model should track the trajectory generated from the swarm model. This will be done as in [12] using dynamic feedback linearization.

B. Dynamic Feedback Linearization

As in [12] we define our linearizing output vector as $\eta = (x_c, y_c)$. Differentiating with respect to time yields

$$\dot{\eta} = \begin{pmatrix}\dot{x}_c \\ \dot{y}_c\end{pmatrix} = \begin{pmatrix}\cos\theta & 0 \\ \sin\theta & 0\end{pmatrix}\begin{pmatrix}v_c \\ \omega\end{pmatrix} \tag{42}$$

We need to differentiate once again as only v_c affects (42) and we need both inputs for controlling (41). Adding an integrator on the linear velocity input as $v_c = \xi_c, \dot{\xi}_c = a$ and differentiating (42) further we obtain

$$\ddot{\eta} = \begin{pmatrix}\cos\theta & -\xi_c\sin\theta \\ \sin\theta & \xi_c\cos\theta\end{pmatrix}\begin{pmatrix}a \\ \omega\end{pmatrix} \tag{43}$$

Defining the new input (a, ω) as

$$\begin{pmatrix}a \\ \omega\end{pmatrix} = \begin{pmatrix}\cos\theta & \sin\theta \\ \dfrac{-\sin\theta}{\xi_c} & \dfrac{\cos\theta}{\xi_c}\end{pmatrix}\begin{pmatrix}u_1 \\ u_2\end{pmatrix} \tag{44}$$

and (u_1, u_2) as

$$\begin{pmatrix}u_1 \\ u_2\end{pmatrix} = \begin{pmatrix}\ddot{x}_i + K_{p1}(x_i - x_c) + K_{d1}(\dot{x}_i - \dot{x}_c) \\ \ddot{y}_i + K_{p2}(y_i - y_c) + K_{d2}(\dot{y}_i - \dot{y}_c)\end{pmatrix} \tag{45}$$

exponentially stabilizing feedback is obtained with $K_{pi} > 0, K_{di} > 0, (i = 1,2)$ The initial state of integrator $\xi_{c0} \neq 0$ and the desired trajectory should be persistent in order to avoid the singularity in (44) when $\xi_c = 0$. For more details to avoid singularities please refer to [12] where the sufficient conditions are discussed in detail.

For the practical implementation the high level swarm controller and the low level WMR controller swarm controller are combined in the following manner.

1) First the swarm model is simulated from time $t = [t_i, t_i + T_{swarm}]$ where t_i is the initial time and T_{swarm} is the update period of the swarm simulation.

2) Next, the outputs from the swarm model from time $t = [t_i, t_i + T_{swarm}]$ are used as the desired trajectories for the low level controller. The outputs from the low level controller are applied input to the WMR for time $t = [t_i, t_i + T_{swarm}]$. The actual position and velocity of the WMR will be calculated.

3) Now the swarm members in the swarm model will be re-initialized with the WMR agents' positions and velocity using the results of Step (2). There will be a difference at time $t = t_i + T_{swarm}$ due to the tracking error.

4) Return to step (1).

This procedure above combines the inner and outer control loops for certain values of T_{swarm}. Furthermore, T_{swarm} is an important parameter for good tracking performance. Additionally, careful adjustment of the gains of both inner loop and outer loop is required. The inner and outer loop controllers normally show good results when the inner loop is significantly faster than the outer loop.

It is important to mention that saturation on control input $\mathbf{u}_i^{ext}$ besides selecting bounded inter individual repulsion function ensures that the generated trajectory during $(t_i, t_i + T_{swarm})$ is a feasible trajectory for practical implementation.

IV. Simulation Results

Swarm of 20 members in 2D space is considered in the first set of simulations. Control allocation without input saturation is considered at this stage. Control allocation can be characterized as the optimization problem given in (31). The SNOPT solver (optimization package) is used to solve the allocation problem. However, in a case that there is no

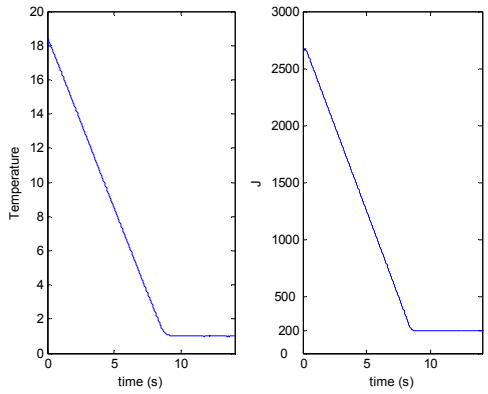

Fig. 2 Regulation of potential function and temperature outputs

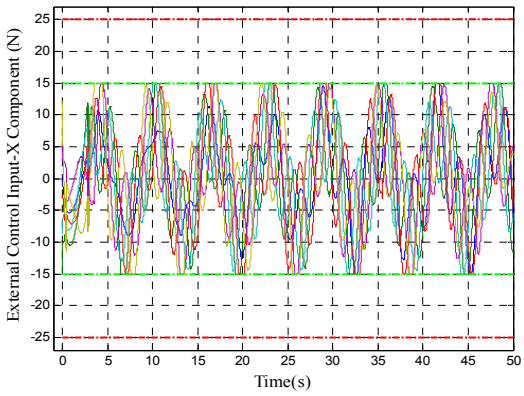

Fig.3 High-level Control Input

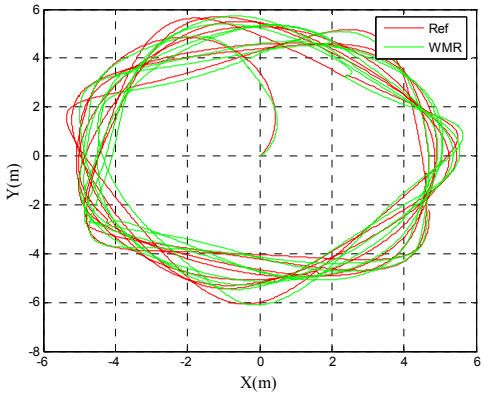

Fig.4 WMR trajectory with disturbance

input saturation, the solution is as same as an analytical solution of the problem, see pseudo inverse solution (32). Fig. 2 shows how temperature and fully potential function are regulated at their respective desired values 1.00 and 200.00. This shows the capability of the proposed scheme to control multi outputs.

The purpose of the second set of simulation is to implement the energetic swarm controller for a group of wheeled mobile robot. Therefore, the swarm with six members moving in 2D is considered. The desired trajectory for the swarm canter is $\bar{x}_{des} = [5.0\cos(t) \quad 5.0\sin(t)]^T$. The disturbance in (1) is $2.0\sin(t)$. It is shown how saturation of control input can be integrated to control allocation algorithm for a practical case. Fig. 3 shows how the high level control input varies. $\mathbf{u}_{i\min}, \mathbf{u}_{i\max}$ are set to -17.0 and 17.0 respectively for all the members in steady state and $+/-25.0$ during the transient phase. In Fig. 4, it can be seen that the lower level controller makes a WMR follow the trajectory generated by the swarm model while a disturbance is applied.

V. Conclusion

In this work we have implemented a swarm controller for multiple control variables using a control allocation approach. The SNOPT solver is used in conjunction with optimization constraints to account for control input saturation. To improve results further a low-level controller is introduced, to enhance WMR trajectory tracking Future work includes a more systematic way to deal with the saturation and to develop a low level controller that is robust.

References

[1] R. Pedrami and B.W. Gordon, "Control of energetic robotic swarm systems," in *Proc. Int. Conference on Robotics and Biomimetics, Sanya,* China, pp.547-552, 2007.

[2] R. Pedrami and B.W. Gordon, "Control and analysis of energetic swarm systems," in *Proc. American Control Conference,* New York, pp. 1894–1899, 2007.

[3] V. Gazi, and K. M. Passino, "A class of attractions/repulsion functions for stable swarm aggregation," *International Journal of Control*, vol. 77, no. 18, pp. 1567-1579, 2004.

[4] V. Gazi and K. M. Passino, "Stability analysis of swarms," in *Proc. 2002 American Control Conference*, Anchorage, pp. 1813–1818, 2002.

[5] J. H. Reif and H. Wang, "Social potential fields: A distributed behavioural control for autonomous robots," *Robotics and Autonomous Systems*, vol. 27, pp. 171–194, 1999.

[6] R. Pedrami and B. W. Gordon, "Control and cohesion of energetic swarms" in *Proc. American Control Conference,* Seattle, 2008, pp. 129-134, 2008.

[7] R. Pedrami and B.W. Gordon, "Control allocation for energetic swarms," CIS Technical Report, Concordia University, Montreal, QC, 2007.

[8] F. Leif, K-Y. Lum, et al, "Constrained nonlinear finite-time control allocation," in *Proc. American Control Conference,* New York, 2007, pp. 3801-3806, 2007.

[9] T. A. Johansen, "Optimizing nonlinear control allocation," in *Proc. 43rd IEEE Confernece on Decision and Control*, Bahamas, pp. 3435-3340, 2004.

[10] T. A. Johansen, T. I. Fossen and P. B. Svein, "Constrained nonlinear control allocation with singularity avoidance using sequential quadratic programming," *IEEE Transactions on Control Systems Technology*, vol. 12, no. 1, pp. 211-215, 2004.

[11] P. Gill, W. Murray and M. Saunders. (2006, 02, 12). *Users Guide for SNOPT 7* [pdf]. Available: http://www.sbsi-sol optimize.com/manuals/SNOPT%20Manual.pdf

[12] G.Oriolo, A.De Luca and M.Vendittelli, "WMR control via dynamic feedback linearization: design, implementation, and experimental validation," *IEEE Transactions on Control Systems Technology*, vol.10, no.6, pp. 835-852, 2002.

[13] A. Regmi, R. Sandoval, R. Byrne, H. Tanner, C. T. Abdallah, "Experimental implementation of flocking algorithm in wheeled mobile robots," Proc. 2005 American Control Conf., vol. 5, pp. 4917-4922, Jun. 2005.